DOPPLER FREQUENCY GEOLOCATION OF UNCOOPERATIVE RADARS

B.H. Lee,Y.T. Chan, and F. Chan,
Dept. of Electrical and Computer Engineering
Royal Military College of Canada
Kingston, Ontario, Canada

Huai-Jing Du and Fred A. Dilkes
Defence Research and Development Canada
Ottawa, Ontario, Canada

ABSTRACT

Passive geolocation of uncooperative radar emitters remains an important problem in radar electronic warfare. Several location estimation techniques have been investigated in the past. In this paper, we present a passive geolocation technique for radar emitters using Doppler frequency measurements. For uncooperative sources, neither the emitter location, nor its transmitted frequency is known a priori. The relationship between these unknowns and the measured Doppler frequencies is non-linear. In the special case where the moving receiver measures frequencies along a straight path at constant speed, the relationship becomes linear in the Cartesian location coordinates. A simple 1-D discrete search for the transmitted frequency is followed by a least squares (LS) estimator to provide a coarse estimate of the emitter coordinates. This is followed by Newton's algorithm to provide a maximum likelihood (ML) estimation. The simulation results demonstrate that the resulting ML estimator approximately meets the Cramer-Rao lower bound (CRLB).

I. INTRODUCTION

An important function in electronic warfare is to determine the position of an uncooperative stationary emitter. Receivers in separate but known positions can measure, depending on the particular applications, the time-difference-of-arrival (TDOA), angle-of-arrival (AOA), signal strengths, or Doppler-shifted frequency (DSF), to localize the emitter [1]. This paper considers the problem of locating a radar that emits a signal with a constant carrier frequency using a single airborne sensor channel. Under such circumstances, neither TDOA- nor TOA-based techniques are applicable, due to insufficient sensor assets and unknown departure times. Additionally, if the receiver does not have an array for AOA measurements, the only alternative is DSF.

In the DSF scenario, one single-channel airborne receiver, which in this paper is an unmanned aerial vehicle (UAV), is required to estimate the location of an uncooperative emitter based on Doppler frequency changes induced by relative motion. The UAV is assumed to make several discrete frequency measurements along its trajectory.

A companion paper [2] gives methods for measuring DSF. When the radar signal is a sequence of pulsed sinusoids, and when the signal-to-noise ratio is low, large errors in DSF measurements may occur. The measured DSF can be equal to the true DSF offset by harmonics of the pulse repetition frequency. This can give rise to significant localization errors. This paper does not consider this situation and assumes the DSF measurements contain only Gaussian noise.

For simplicity, let the radar have coordinates (x, y) be constrained to a two-dimensional plane with z=0. It is rather straightforward to generalize the method in Section II for the case when $z \neq 0$ and is unknown. Denote the carrier frequency of its transmissions by f_0. Since the Doppler frequency measurements depend non-linearly on the unknowns (f_0, x, y), an estimator is proposed based on a multi-modal cost function. Minimization of the cost function generally requires a search over a three-parameter space or iterative minimization. Depending on the initial condition, iteration may converge to a local minimum, or not at all.

In the special case where the UAV makes frequency measurements along a non-maneuvering path of constant course and speed, the measurement equation becomes linear in (x, y) for a fixed f_0. Hence a 1-D search in f_0 can produce least squares (LS) estimates of (x, y) which, together with f_0, can find a solution that minimizes a cost function. This LS technique yields errors that are above the Cramer-Rao lower bound (CRLB) [3]. However, as simulation results demonstrate, the LS is a close initial condition for a Newton's algorithm [4] which produces accuracy that closely approaches the CRLB.

Under many circumstances, the requirement of obtaining three or more measurements only during non-maneuvers is not very restrictive. An aircraft will normally have short (or longer depending on scenarios) non-maneuvering durations. It is a simple matter of grouping together segments of three or more measurements, with each segment coming from a non-

1-4244-1513-06/07/$25.00 ©2007 IEEE

maneuvering period. Nevertheless, generalized techniques that apply to manoeuvrable receiver platforms such as tactical jet aircraft with highly non-linear trajectories are also possible. These are expected to require greater computational complexity.

In the following, Section II develops the localization equations, and formulates the LS linear equation for (x, y), followed by the Newton's algorithm in Section III. Section IV gives the simulation results. The conclusions are in Section V.

II. PROBLEM FORMULATION AND SOLUTION

Doppler-shifted frequencies are measured at N separate instants along the UAV trajectory. At the i-th instant, the exact Doppler-shifted frequency is given by [1]

$$f_i(f_0, x, y) = f_0\left(1 + \frac{V\cos\alpha_i}{c}\right), \quad i = 1,\ldots,N \qquad (1)$$

where f_0 represents the transmitted frequency by the stationary emitter, V is the speed of the UAV, and c is the propagation speed of signal. The variable α_i represents the angle between the UAV's velocity vector and the direction vector from the UAV to the emitter, whose position is specified by x and y, as indicated in Figure 1.

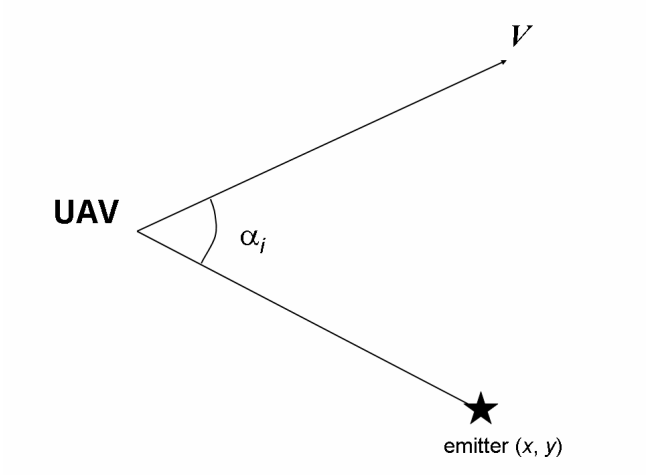

Figure 1: UAV-Emitter Geometry.

The measured Doppler frequency is given by

$$\tilde{f}_i = f_i + e_i \qquad (2)$$

where e_i denotes the measurement noise, and is a zero mean, independently and identically distributed (i.i.d.) Gaussian random variable of variance σ^2.

The emitter position is at (x, y) and the UAV positions are (x_i, y_i, z_i), i = 1,….,N. The UAV has a known position vector

$$\vec{P}_i = x_i\vec{x} + y_i\vec{y} + z_i\vec{z}\,, \qquad (3)$$

and a known velocity vector

$$\vec{V} = V_x\vec{x} + V_y\vec{y} + V_z\vec{z}\,. \qquad (4)$$

The emitter position vector is

$$\vec{P}_e = x\vec{x} + y\vec{y}\,. \qquad (5)$$

In (3)-(5) $\vec{x}, \vec{y}, \vec{z}$ are mutually orthogonal unit vectors for the 3-D rectangular coordinate system. Given $\tilde{f}_i, \vec{P}_i$, $i = 1,\ldots,N$, and $\vec{V}$, the problem is to estimate f_0, x, y.

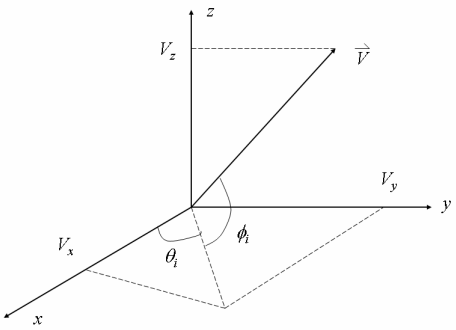

Figure 2: Components of the UAV velocity vector.

From Figure 2, with $V = |\vec{V}|$,

$$\left.\begin{aligned} V_x &= V\cos\phi_i\cos\theta_i \\ V_y &= V\cos\phi_i\sin\theta_i \\ V_z &= V\sin\phi_i \end{aligned}\right\} \qquad (6)$$

where θ_i is the azimuth heading (w.r.t. x-axis) and ϕ_i is the elevation heading (w.r.t. x-y plane).

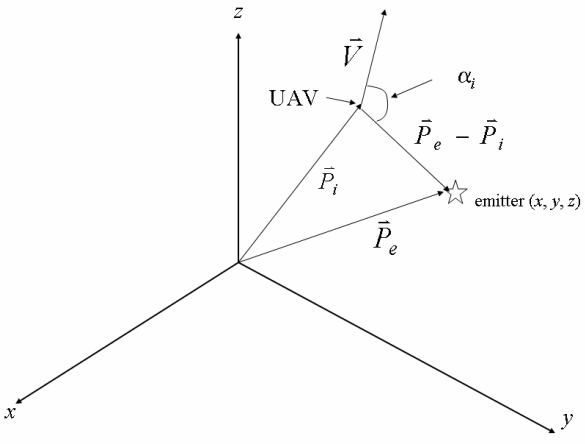

Figure 3: UAV-emitter vectors.

Then from Figure 3, the inner product

$$\vec{V}\cdot(\vec{P}_e-\vec{P}_i)=VR_i\cos\alpha_i \tag{7}$$

where

$$R_i=\left|\vec{P}_e-\vec{P}_i\right| =\sqrt{(x-x_i)^2+(y-y_i)^2+(z-z_i)^2} \tag{8}$$

Substituting (6) and (8) into (7) with $z = 0$ yields

$$R_i\cos\alpha_i-k_i=b_ix+c_iy \tag{9}$$

where

$$\left.\begin{aligned} b_i&=\cos\phi_i\cos\theta_i\\ c_i&=\cos\phi_i\sin\theta_i\\ d_i&=\sin\phi_i\\ k_i&=-[x_ib_i+y_ic_i+z_id_i]\end{aligned}\right\} \tag{10}$$

Suppose the UAV is on a non-maneuvering path at measurement instants i=1, 2, 3, …,N , for $N \geq 3$.

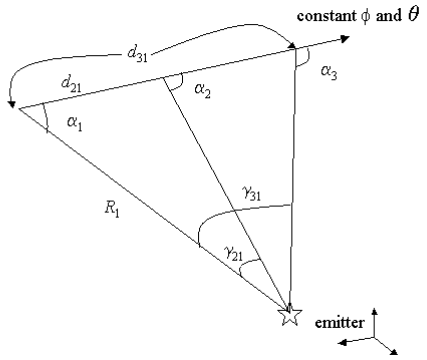

Figure 4: A non-maneuvering UAV.

From Figure 4, applying the sine law gives

$$\frac{d_{21}}{\sin\gamma_{21}}=\frac{R_1}{\sin\alpha_2} \tag{11}$$

$$\frac{d_{i1}}{\sin\gamma_{i1}}=\frac{R_i}{\sin\alpha_1},\quad i=2,3,\ldots,N \tag{12}$$

The distance between the UAV at positions $i=2,3,....,N$ and $i=1$ is denoted by $d_{i1}=\left|\vec{P}_i-\vec{P}_1\right|$. The angle subtended by the emitter to the UAV positions is γ_{i1}. It is clear from Figure 4 that

$$\gamma_{i1}=\alpha_i-\alpha_1,\quad i\geq 2 \tag{13}$$

Now (11), (12) and (13) give

$$R_1=\frac{d_{21}\sin\alpha_2}{\sin(\alpha_2-\alpha_1)} \tag{14}$$

$$R_i=\frac{d_{i1}\sin\alpha_1}{\sin(\alpha_i-\alpha_1)},\quad i=2,...,N \tag{15}$$

The matrix equation from (9), for $i = 1,…, N$, is

$$\mathbf{A}\boldsymbol{\mu}=\mathbf{B} \tag{16}$$

where

$$\boldsymbol{\mu}=\begin{bmatrix}x\\ y\end{bmatrix}, \tag{17}$$

$$\mathbf{A}=\begin{bmatrix}b_1 & c_1\\ \vdots & \vdots\\ b_N & c_N\end{bmatrix}, \tag{18}$$

and

$$\mathbf{B}=\begin{bmatrix}R_1\cos\alpha_1-k_1\\ \vdots\\ R_N\cos\alpha_N-k_N\end{bmatrix}. \tag{19}$$

The LS solution is

$$\boldsymbol{\mu}=(\mathbf{A}^T\mathbf{A})^{-1}\mathbf{A}^T\mathbf{B} \tag{20}$$

The preceding equations are used to develop the following 1-D search and LS algorithm:

(i) Establish a range for f_0 from $\tilde{f}_a-\Delta$ to $\tilde{f}_a+\Delta$ where $\tilde{f}_a$ is the simple average of the N measurements $\tilde{f}_i$, and $\Delta\approx\tilde{f}_aV/c$ is the maximum frequency shift that the DSF can have, given a known UAV speed V.

(ii) Beginning with $\hat{f}_0=\tilde{f}_a-\Delta$, find an estimate of α_i, $i = 1,…,N$ from (1), with $\hat{f}_0$ replacing f_0 and $\tilde{f}_i$ replacing f_i. Determine an estimate of R_i from α_i using (14) and (15). Then compute the elements of **A** in (18) and **B** in (19). Then compute an estimate for $\boldsymbol{\mu}$ using (20).

(iii) Using the estimate for (x, y), find new estimates of R_i and α_i from (8) and (9). Use these values to find predicted Doppler frequencies, denoted by $\hat{f}_i$, from (1).

(iv) Evaluate the cost function

$$\rho = \sum_{i=1}^{N} \left(\hat{f}_i - \tilde{f}_i \right)^2 \qquad (21)$$

(v) Increment $\hat{f}_0$ by one step in frequency (using a frequency granularity of, for example, 5Hz) and repeat (ii) to (v) until $\hat{f}_0 = \tilde{f}_a + \Delta$.

(vi) Pick the $\hat{f}_0, x, y$ that give the minimum cost ρ in (21).

Simulation results indicate that the LS estimates have errors that are higher than the CRLB. However, they are close initial conditions for the Newton's algorithm.

III. NEWTON'S ALGORITHM

Let the ML function be

$$J(\boldsymbol{\beta}) = \sum_{i=1}^{N} \left(f_i(\boldsymbol{\beta}) - \tilde{f}_i \right)^2 \qquad (22)$$

where

$$\boldsymbol{\beta} = [f_0 \quad x \quad y]^T \qquad (23)$$

and the dependence of f_i on $\boldsymbol{\beta}$ is a consequence of (1).

The Newton's algorithm is [4]

$$\boldsymbol{\beta}^{(n+1)} = \boldsymbol{\beta}^{(n)} - \left(\nabla^2 J\left(\boldsymbol{\beta}^{(n)}\right) \right)^{-1} \nabla J\left(\boldsymbol{\beta}^{(n)}\right) \qquad (24)$$

Here $\boldsymbol{\beta}^{(n)}$ represents the n-th approximation of $\boldsymbol{\beta}$, $\nabla J(\boldsymbol{\beta})$ represents the vector of first partial derivatives of $J(\boldsymbol{\beta})$ with respect to the components of $\boldsymbol{\beta}$, and $\nabla^2 J(\boldsymbol{\beta})$ represents the matrix of second partials. The requisite partial derivatives are given in Appendix B.

IV. SIMULATION RESULTS

In the simulation experiment the emitter is at $(x, y) =$ (5000, 5000) meters, the transmitted carrier frequency is $f_0 = 1 \times 10^{10}$ Hz, and $c = 3 \times 10^8$ m/s. The UAV, traveling with speed V=100m/s, follows three different non-maneuvering segments, making 6 Doppler frequency measurements at 10 second intervals during each segment for a total of $N = 3 \times 6 = 18$ measurements. The first segment begins at $(x_1, y_1, z_1) = (0,0,1000)$ and the orientation of the velocity vector is defined by: $\theta_i = 60^\circ, \phi_i = 10^\circ$. The second segment starts at $(x_7, y_7, z_7) = (3000,5000,2000)$ and is defined by $\theta_i = 45^\circ, \phi_i = -5^\circ$. The third segment begins at $(x_{13}, y_{13}, z_{13}) = (7000,8000,1500)$ and is defined by $\theta_i = 270^\circ, \phi_i = 0^\circ$. The complete flight path is shown in Figure 5.

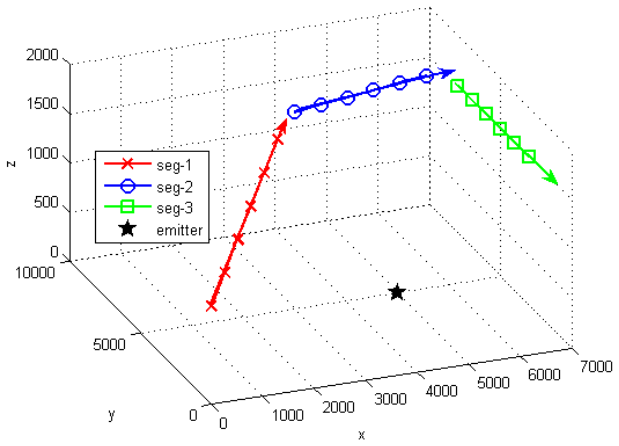

Figure 5: UAV flight path.

For 100 independent trials with σ varying from 1 to 10Hz, the root-mean-square-error (RMSE), for example for the estimate $\hat{f}_0$, is

$$\mathrm{RMSE}(f_0) = \sqrt{\frac{\sum_{i=1}^{100} \left(\hat{f}_0(i) - f_0 \right)^2}{100}} \qquad (25)$$

where $\hat{f}_0(i)$ indicates the estimate for f_0 during the i-th trial.

RMSE plots for f_0, x and y are shown in Figures 6-8 along with the CRLB given in Appendix A. They show that the LS RMSE cannot meet the $[\mathrm{CRLB}]^{1/2}$. However, the LS estimate can provide close initial conditions for Newton's algorithm, whose RMSE is close to $[\mathrm{CRLB}]^{1/2}$. Initial conditions that are far away from the true $\boldsymbol{\beta}$ of (23) have also been simulated, and the Newton's algorithm failed to converge in those cases.

In the simulation experiment, there is no solution ambiguity, i.e., uncertainty concerning which side the radar is with respect to the UAV path. This is because the UAV changes directions between non-maneuvering paths. The number of measurements, N, is arbitrary. A larger N will give a more accurate solution, as the CRLB decreases with increasing N. This method requires a minimum of two different non-maneuvering segments with 2 Doppler measurements for a total of $N = 2 \times 2 = 4$ measurements.

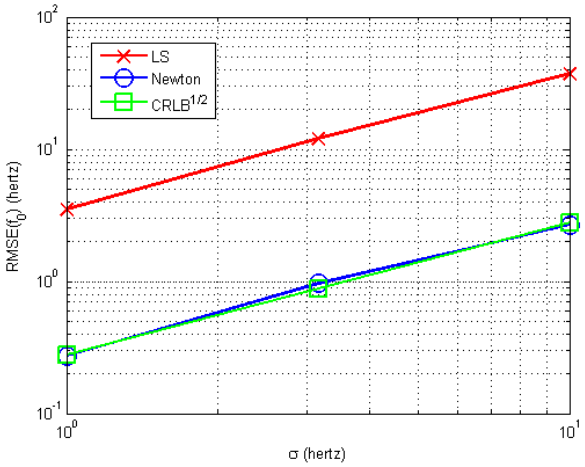

Figure 6: RMSE for f_0.

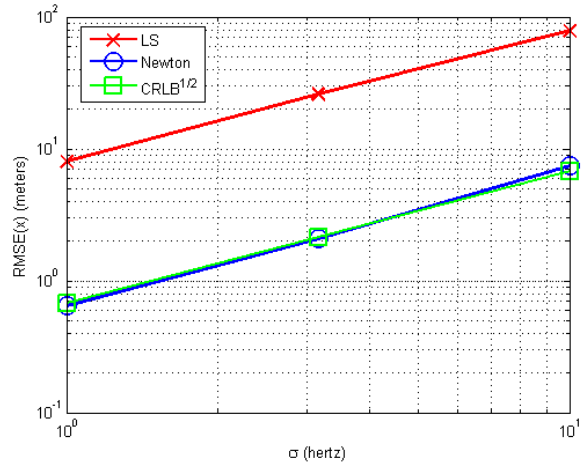

Figure 7: RMSE for x.

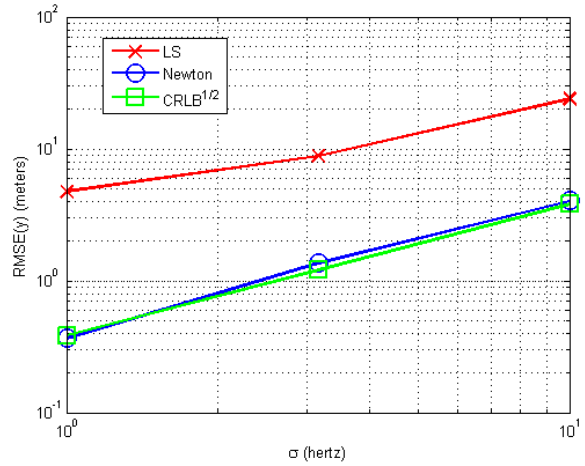

Figure 8: RMSE for y.

V. CONCLUSIONS

A novel localization method that meets the Cramer-Rao lower bound has been presented. The localization of an emitter, by Doppler-shifted frequencies, is a nonlinear problem and requires a 3-D minimization. Because of a multi-modal cost function, proper initial conditions are important for any iterative search algorithm, to ensure convergence and convergence to the global minimum

A mild restriction that the UAV be non-maneuvering over measurement segments results in linear equations and LS estimates. Although the accuracy is not what is theoretically achievable, the LS estimates, since they are close to the true values, provide good initial conditions for the Newton's algorithm, which then produces estimates that meet the CRLB.

This problem can be easily extended to the case where the elevation of the target is unknown, i.e., the unknowns are (f_0, x, y, z).

REFERENCES

[1] D.J. Torrieri, "Statistical Theory of Passive Location Systems,'' IEEE AER-20, 183-198, March 1984.

[2] J. Gai, F. Chan, Y.T. Chan, H.J. Du, F.A. Dilkes, "Frequency Estimation of Uncoopera-tive Coherent Pulse Radars,'' MILCOM, 2007.

[3] H. Van Trees, *Detection, Estimation and Modulation Theory Part I*, Wiley, Toronto, 1968.

[4] C.W. Helstrom, *Statistical Theory of Signal Detection*, Pergamon Press, Toronto 1968.

APPENDIX

A. CRLB

From (2), the measured Doppler frequency is

$$\tilde{f}_i = f_i + e_i, \quad i = 1,\ldots,N \tag{A.1}$$

In the case where e_i are Gaussian, zero mean and i.i.d. random noise variables, the log likelihood function [2] is

$$J(f_0, x, y) = \sum_{i=1}^{N} \left(f_i(f_0, x, y) - \tilde{f}_i \right)^2 \tag{A.2}$$

The Fisher Information matrix (FIM) is

$$\mathbf{FIM} = \frac{1}{\sigma^2} \mathbf{G}\mathbf{G}^T \tag{A.3}$$

where

$$\mathbf{G} = \begin{bmatrix} \frac{\partial f_1}{\partial f_0} & \cdots & \frac{\partial f_N}{\partial f_0} \\ \frac{\partial f_1}{\partial x} & \cdots & \frac{\partial f_N}{\partial x} \\ \frac{\partial f_1}{\partial y} & \cdots & \frac{\partial f_N}{\partial y} \end{bmatrix}. \quad \text{(A.4)}$$

The CRLB for the three unknowns is determined from the inverse of the Fisher Information matrix,

$$\mathbf{FIM}^{-1} = \begin{bmatrix} \mathrm{CRLB}(f_0) & & \\ & \mathrm{CRLB}(x) & \\ & & \mathrm{CRLB}(y) \end{bmatrix}. \quad \text{(A.5)}$$

B. PARTIAL DERIVATIVES

This section contains all the partial derivatives required for calculating the CRLB and the Newton's algorithm of (24).

$$\frac{\partial f_i}{\partial f_0} = \left(1 + \frac{V \cos\alpha_i}{c}\right) \quad \text{(A.6)}$$

$$\frac{\partial f_i}{\partial x} = \frac{f_0 V}{c}\left(\frac{b_i}{R_i} - \frac{(x_i - x)\cos\alpha_i}{R_i^2}\right) \quad \text{(A.7)}$$

$$\frac{\partial f_i}{\partial y} = \frac{f_0 V}{c}\left(\frac{c_i}{R_i} - \frac{(y_i - y)\cos\alpha_i}{R_i^2}\right) \quad \text{(A.8)}$$

where

$$\cos\alpha_i = \frac{b_i x + c_i y + k_i}{R_i} \quad \text{(A.9)}$$

and

$$R_i = \sqrt{(x - x_i)^2 + (y - y_i)^2 + (-z_i)^2} \quad \text{(A.10)}$$

For Newton's method

$$\nabla J(\boldsymbol{\beta}) = \begin{bmatrix} \frac{\partial J}{\partial f_0} & \frac{\partial J}{\partial x} & \frac{\partial J}{\partial y} \end{bmatrix}^T \quad \text{(A.11)}$$

and

$$\nabla^2 J(\boldsymbol{\beta}) = \begin{bmatrix} \frac{\partial^2 J}{\partial f_0^2} & \frac{\partial^2 J}{\partial f_0 \partial x} & \frac{\partial^2 J}{\partial f_0 \partial y} \\ \frac{\partial^2 J}{\partial x \partial f_0} & \frac{\partial^2 J}{\partial x^2} & \frac{\partial^2 J}{\partial x \partial y} \\ \frac{\partial^2 J}{\partial y \partial f_0} & \frac{\partial^2 J}{\partial y \partial x} & \frac{\partial^2 J}{\partial y^2} \end{bmatrix}. \quad \text{(A.12)}$$